ChemComm

COMMUNICATION

View Article Online
View Journal | View Issue

Cite this: *Chem. Commun.*, 2017, 53, 1743

Received 11th October 2016,
Accepted 3rd January 2017

DOI: 10.1039/c6cc08204a

www.rsc.org/chemcomm

Construction and characterisation of a heparan sulphate heptasaccharide microarray†

Jianhong Yang,[ab] Po-Hung Hsieh,[a] Xinyue Liu,[c] Wen Zhou,[ad] Xing Zhang,[c] Jing Zhao,[c] Yongmei Xu,[a] Fuming Zhang,[c] Robert J. Linhardt[c] and Jian Liu*[a]

A targeted heptasaccharide library was synthesised to prepare a heparan sulphate (HS) microarray. The array was probed with two glycan-binding proteins, HS 3-*O*-sulphotransferase 1 and antithrombin, demonstrating the binding selectivity between HS and proteins. The HS microarray technique will accelerate the understanding of the structure and function relationships of HS.

HS plays important physiological and pathophysiological roles, including embryonic development, inflammatory responses, blood coagulation and viral/bacterial infections.[1–3] In particular, heparin, a special form of HS containing higher sulphation and IdoA levels, is commonly used in clinics for the treatment of patients with thrombotic disorders.[4] HS exhibits biological activities through its interactions with proteins. The selectivity is largely governed by the sulphation patterns in HS.[5] HS includes sulphation at the 2-OH of IdoA (and to a lesser extent GlcA) and the *N*-, 3-OH and 6-OH positions of GlcN residues. Among these sulphation types, the 3-*O*-sulphation of GlcN is the least abundant structural motif in HS. It is noteworthy, however, that 3-*O*-sulphation is carried out by one of seven different 3-*O*-sulphotransferase isoforms, suggesting that this rare modification might significantly impact the biologically relevant HS fine-structure.[6] The size of the sulphated saccharide domain also plays critical roles in displaying high binding affinity to a particular protein. The size to display the biological activity varies in the range of pentasaccharide (5-mer), binding to a single compact protein, to an octadecasaccharide (18-mer), binding to a larger extended protein or to a protein complex.[7]

Glycan microarray technologies have become a powerful method to investigate glycan–protein interactions.[8–12] A number of defined neutral and sulphated saccharides have been made for glycan microarrays through an NIH sponsored consortium (www.functionalglycomics.org). The improvement of methods used to isolate, purify and synthesise new classes of saccharides will further expand the structural diversity in glycan microarrays.[13–16] Recently, a microarray of glycans from plants was reported.[17] Glycan microarrays containing strongly acidic oligosaccharides such as those from HS, however, have lagged behind, while a chondroitin sulphate tetrasaccharide array has been reported.[18] An HS microarray was reported, but the array covered a mixture of oligosaccharides or polysaccharides.[19,20] The Seeberger group pioneered the development of the structurally defined HS-microarray.[21,22] However, only a small number of tetrasaccharides and hexasaccharides were present on their array, underrepresenting the HS glycome. An HS microarray containing eight HS hexasaccharides obtained *via* chemoenzymatic methods was recently reported that, however, did not contain 3-*O*-sulphated structures.[23]

A reasonably diversified collection of oligosaccharides is required to construct an HS microarray for widespread use in biological studies. To this end, a library of HS oligosaccharides containing 21 HS oligosaccharides (**1–21**) was synthesised using a chemoenzymatic approach[24,25] (Fig. 1). Compounds **1–14** were utilised for the array analysis by affixing on the array slides through an amino group at the reducing ends. The oligosaccharide synthesis was initiated from a monosaccharide using a glycosyltransferase, an epimerase and different sulphotransferases (ESI,† Fig. S1). The azido group at the reducing end of each oligosaccharide was reduced to the primary amino group by hydrogenation in the last step of each synthesis to afford the final products, **1–14**. Similar sulphation patterns present in heptasaccharides are found in the HS isolated from mouse or human tissues.[26,27] Approximately 5–10 mg of each oligosaccharide were prepared. The structures were confirmed by high-resolution mass spectrometry (MS) (ESI,† Table S1) and ^{1}H- and ^{13}C-NMR (ESI,† Fig. S3–S44).

Seven fluorescently labelled octasaccharides (compounds **15–21**) were synthesised from appropriate precursors (ESI,† Fig. S2)

[a] *Division of Chemical Biology and Medicinal Chemistry, Eshelman School of Pharmacy, University of North Carolina, Chapel Hill, NC 27599, USA. E-mail: jian_liu@unc.edu*
[b] *College of Environmental & Safety Engineering, Changzhou University, Changzhou 213164, Jiangsu, China*
[c] *Department of Chemistry and Chemical Biology, Centre for Biotechnology and Interdisciplinary Studies, Rensselaer Polytechnic Institute, Troy, New York 12180, USA*
[d] *School of Chinese Medical Material, Guangzhou University of Chinese Medicine, Guangzhou, 510006, Guangdong, China*

† Electronic supplementary information (ESI) available. See DOI: 10.1039/c6cc08204a

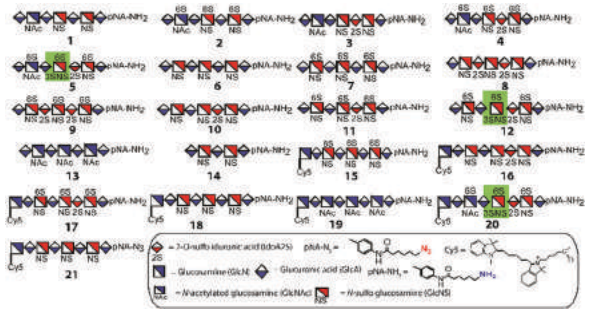

Fig. 1 Symbolic structures of compounds synthesised for this study. Keys for each symbol are shown in the box. For clarity, the sites of 3-*O*-sulphation in the 3-*O*-sulpho group containing oligosaccharides are highlighted with a green box. pNA-NH_2 and pNA-N_3 represent *N*-(6-aminohexanamidyl) *p*-aminophenyl and *N*-(6-azidohexanamidyl) *p*-aminophenyl groups, respectively.

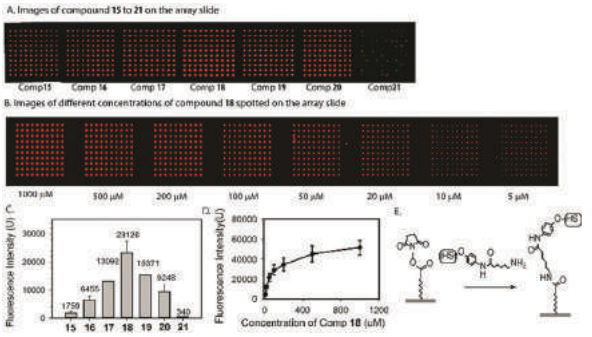

Fig. 2 Oligosaccharides on the surface of array slides. Panel A shows the images of compounds **15–21** on the array slide. Panel B shows the images of array slides spotted with different concentrations of compound **18**. Panel C shows the digitised analysis of the images from compounds **15–21**. The values for fluorescence intensity are displayed above each bar graph. The local background of the fluorescence value is 9 ± 5. Panel D shows the correlation curve of the fluorescence intensity and the spotted concentrations of compound **18**. Panel E shows the chemical reaction involved in the affixation process. The intensity data are the mean value ± S.D. of 100 individual spots.

carrying a fluorescent tag (Cy5) at their non-reducing end. Compounds **15–20** have a primary amino group at their reducing end. Compound **21** has an azido group at its reducing end. Each fluorescently labelled octasaccharide was converted from the precursor heptasaccharide through three reaction steps. For example, compound **15** has a nearly identical carbohydrate structure to compound **7**, with the exception that it has an extra glucosamine residue and a Cy5 tag at its non-reducing end. Compounds **16**, **17**, **18**, **19** and **20** were synthesised from the azido compounds **10**, **11**, **6**, **13** and **5**, respectively. The conversion of the azido group to the primary amino group in compounds **15–20** used triphenylphosphine. The structures of compounds **15–21** were confirmed by MS analysis (ESI,† Table S1).

We utilised six fluorescently labelled oligosaccharides (**15–20**) and assessed the consistency of oligosaccharide immobilisation on the array through the measurement of fluorescence intensity. The surface of the array slide is functionalised with *N*-hydroxysuccinimide (NHS) groups that react with the primary amino group present at the reducing end of the oligosaccharide (Fig. 2E). Six different oligosaccharides in a total of 100 spots, for each compound, were printed on the array slide to examine the variability in affixation efficiency on the slide surface. The fluorescence intensity for each spot of an individual compound was very similar (Fig. 2A), suggesting the chemistry was consistent. Compound **21** displayed a 68-fold lower fluorescence intensity than compound **18** due to the lack of an amino group at its reducing end (Fig. 2C). The affixation of oligosaccharides was, therefore, accomplished through a reaction of the primary amino group on the glycan's reducing end and the NHS activated carboxyl group on the microarray slide. In contrast, the intensity across substrates was unevenly displayed (Fig. 2C). One plausible explanation is that the fluorescence was differentially quenched. Alternatively, different sulphated oligosaccharides may display different immobilisation efficiencies on the slide surface.

Next, we demonstrated the relationship between the amount of oligosaccharides on the array chip and the concentration of the printed oligosaccharide. Serially diluted compound **18**, at a range of concentrations from 5 to 1000 μM, were spotted on the array surface. The images demonstrated that the amount of oligosaccharides on the chip correlated with the concentration of loaded oligosaccharide (Fig. 2B), as did the results from digitised analysis of the fluorescence signals (Fig. 2D). A linear correlation was observed in the range of 5–50 μM. In addition to compound **18**, other fluorescently labelled oligosaccharides (compounds **15**, **16**, **17**, **19** and **20**) exhibited similar linear relationships between the amount of oligosaccharide on the chip surface and the concentrations of the oligosaccharides (ESI,† Fig. S45–S47). These results demonstrate the control in affixing HS oligosaccharides on the array slide.

We sought to determine the amount of oligosaccharides on the HS-array slides. Results of using fluorescently labelled oligosaccharides did not offer the amount of the oligosaccharides on the slides. Knowing the amount of the oligosaccharide at the microarray spots is an important indicator for the quality of the array slide. Measuring the amount of oligosaccharide on the slide is challenging due to the extremely small quantity. A cocktail of three heparin lyases was used to degrade the oligosaccharide from hundreds of spots from the surface array slide. Determining the amount of disaccharides liberated by heparin lyase-treatment allowed us to estimate the quantity of the oligosaccharide on the array surface (Fig. 3). The detection of compound **4** on the slide surface, with fluorescently labelled 3-*O*-sulphotransferase 1 (3-OST-1) (Fig. 3A), could also be eliminated through the treatment of heparin lyases (Fig. 3A). The heparin lyase-treatment of the surface bound compound **4** should liberate two disaccharides, as illustrated in Fig. 3B. Indeed, two disaccharides were detected from the analysis of compound **4** digest: ΔUA-GlcNS6S (dp2,NS6S) from internal cleavage and GlcA-GlcNAc6S (dp2,6S) from the non-reducing end (NRE) (Fig. 3D).[28] A known amount of compound **4** was used as an external standard (Fig. 3C). The amount of NRE 6S disaccharide was found to be equivalent to 1.3 ng of compound **4** from 833 spots, and the amount of internal NS6S disaccharide was found to be equivalent to 14 ng of compound **4** from same

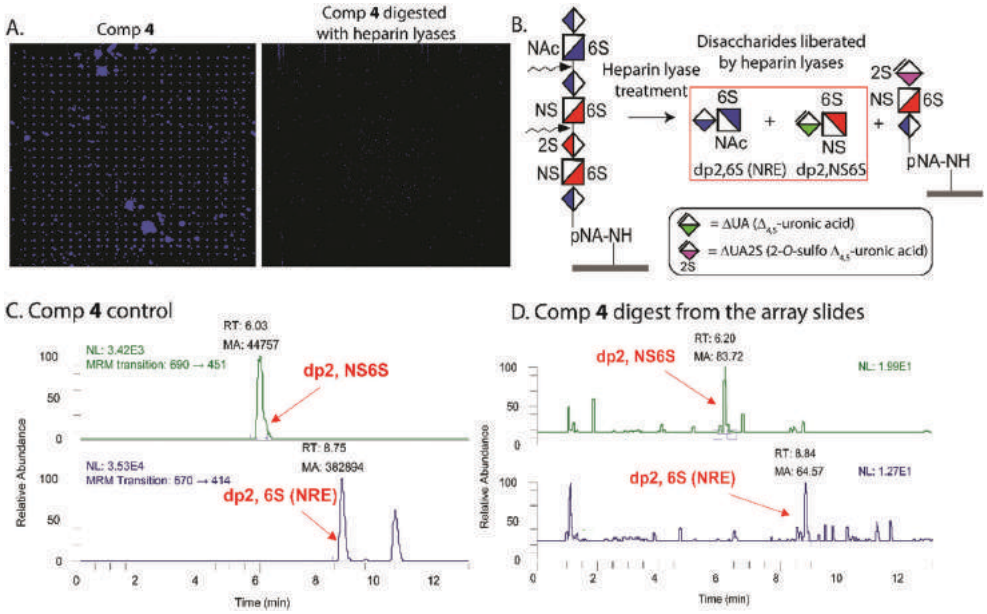

Fig. 3 Quantification of compound **4** on the array surface. Panel A shows the images of the array slides with or without treatment with heparin lyases. The slides were hybridised with Alexa 488 labelled 3-OST-1. Heparin lyase-treatment abolished the binding of 3-OST-1 to the slide. Panel B shows the reaction involved in the degradation of compound **4** by heparin lyases. Cleavage sites of heparin lyases are depicted by waved arrows. Panel C shows the multiple reaction monitoring (MRM) tandem mass spectrometry chromatograms of two disaccharides from the degradation of compound **4** by heparin lyases. Panel D shows the MRM tandem mass spectrometry chromatograms of two liberated disaccharides from the array slide after the treatment with heparin lyases. The quantitative analysis was conducted by comparing the areas of disaccharide signals of ΔUA-GlcNS6S (dp2,NS6S) and GlcA-GlcNAc6S (dp2,6S NRE) from MRM analysis between heparin lyase digested compound **4** and on-site heparin lyase digestion from the array surface covered by compound **4**. From the analysis of digested compound **4** (7.7 μg), the peak area for NS6S was 44 757 and the peak area for 6S was 382 894. From the analysis of the on-site digested surface that consisted of 833 spots, the peak area for NS6S was 83.7, and the peak area for 6S was 64.6. The calculated amount for compound **4** on the surface based on dp2,NS6S was 17 pg per spot (=83.7/44 757 × (7.7 × 10^6)/833). Using a similar method, the calculated amount for compound **4** on the surface based on dp2,6S NRE was 1.6 pg per spot (=64.6/382 894 × (7.7 × 10^6)/833).

number of spots. These results suggest that the amount of compound **4** at each array spot was between 1.6 and 17 pg, or the immobilisation efficiency was estimated to be 1–10%. This 10-fold deviation in the amount of oligosaccharide determination

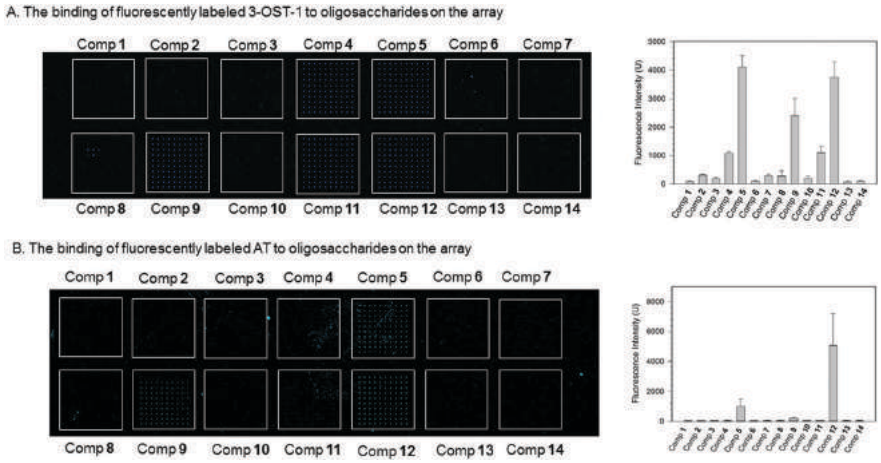

Fig. 4 Images of HS-array analysis. Panel A shows the image of the array slide hybridised with fluorescently labelled 3-OST-1. A total of 14 oligosaccharides were affixed on the slide, and each compound was spotted up to 100 spots. The histogram of fluorescence intensity analysis is shown on the right. The local background of the fluorescence value was to 106 ± 10. Panel B shows the image of the array slide hybridised with fluorescently labelled AT. The local background of the fluorescence value was 60 ± 3. The histogram of fluorescence intensity analysis is shown on the right. Both 3-OST-1 and AT were labelled with Alexa Fluo® 488. The images were acquired using the excitation wavelength of 488 nm on a GenePix 4300 A scanner.

is likely due to either the incomplete digestion of compound **4** from the array slide or the disaccharide products were partially absorbed on the slide surface, resulting in lower quantification. Using the same method, we also determined the amount of compound **1** on the array slide (ESI,† Fig. S48). Disaccharide analysis detected the amount of ΔUA-GlcNS (dp2,NS) disaccharide to be equivalent to 2.8 ng of compound **1** from 830 spots, corresponding to 3.4 pg per spot, or the immobilisation efficiency was estimated to be 2.5%.

The HS microarray was next implemented to probe for binding to proteins. Compounds **1–14** were spotted on the array slides followed by hybridisation with fluorescently labelled proteins. Two proteins, 3-*O*-sulphotransferase isoform 1 (3-OST-1) and antithrombin (AT), were included in the study. 3-OST-1 is an enzyme in the HS biosynthetic pathway that is responsible for introducing a 3-*O*-sulpho group to the HS.[29] Fluorescently labelled 3-OST-1 binds strongly with compounds **5**, **9**, and **12** (Fig. 4A), and has lower binding with **4** and **11**. The results are consistent with the anticipated selectivity to the saccharide sequence based on the co-crystal structures of 3-OST-1.[30] Using surface plasmon resonance (SPR), we confirmed the binding of **5**, **9** and **12** to 3-OST-1 (ESI,† Table S2), but not of **4** and **11**. The undetected binding for **4** and **11** by SPR was probably because the binding affinity of **4** and **11** to 3-OST-1 is low. Next, AT was used to probe the array slide. AT is an inhibitor of factor Xa (FXa) and other proteases in the coagulation cascade; heparin exhibits anti-FXa activity by binding to AT. AT primarily bound to two oligosaccharides, compounds **5** and **12** (Fig. 4B). Among the oligosaccharides on the array, only compounds **5** and **12** contain 3-*O*-sulpho groups, consistent with previous studies, showing that the interaction between HS and AT requires 3-*O*-sulphation.[31,32] The SPR analysis confirmed the microarray analysis (ESI,† Table S2). In the measurement of anti-FXa activity, only compounds **5** and **12** inhibited the activity of FXa (ESI,† Fig. S49), suggesting that the bindings of **5** and **12** to AT mimic heparin's display of anticoagulant activity.

In summary, we demonstrate the construction and characterisation of an HS heptasaccharide microarray. It is crucially important to include sufficiently large oligosaccharides that cover a wide range of sulphation patterns to systematically study HS–protein interactions. In the past, the chemical synthesis of HS oligosaccharides larger than hexasaccharides has been proven to be very difficult. Critical for the success of this study was our ability to synthesise a heptasaccharide library using a highly efficient chemoenzymatic method. This method allowed us to synthesise a relatively large and diverse collection of HS oligosaccharides that can be easily re-synthesised when a microarray hit requires confirmation by other techniques, such as NMR binding studies, X-ray co-crystallography or *in vitro* and *in vivo* biological investigations. The use of fluorescently labelled oligosaccharides and highly sensitive disaccharide analysis by LC/MS enabled the characterisation of this HS microarray. In the future we plan to expand the coverage of the HS microarray to larger oligosaccharides and more diversified sulphated saccharide sequences resembling the structures of HS polysaccharides isolated from natural sources. This well-controlled and representative HS microarray technique should provide a reliable tool for the investigation of the structure and biological function relationship of HS.

JL and YX are founders of Glycan Therapeutics, LLC. Other authors declare no conflict of interest.

The authors thank Dr James Paulson (the Scripps Research Institute) for the help in the initial development of the HS-microarray technique.

References

1 D. Xu and J. Esko, *Annu. Rev. Biochem.*, 2014, **83**, 129.
2 D. Xu, J. Olson, J. N. Cole, X. M. van Wijk, V. Brinkmann, A. Zychlinsky, V. Nizet, J. D. Esko and Y. C. Chang, *Infect. Immun.*, 2015, **83**, 3648.
3 V. N. Patel, I. M. A. Lombaert, S. N. Cowherd, N. Shworak, Y. Xu, J. Liu and M. P. Hoffman, *Dev. Cell*, 2014, **29**, 662.
4 A. Szajek, E. K. Chess, K. Johanssen, G. Gratzl, E. Gray, R. J. Linhardt, J. Liu, T. Morris, B. Mulloy, M. Nasr, Z. Shriver, P. Torralba, C. Viskov, R. Williams, J. Woodcock, W. Workman and A. Al-Hakim, *Nat. Biotechnol.*, 2016, **34**, 625.
5 J. Kreuger, D. Spillmann, J.-P. Li and U. Lindahl, *J. Cell Biol.*, 2006, **174**, 323.
6 B. Thacker, D. Xu, R. Lawrence and J. Esko, *Matrix Biol.*, 2014, **35**, 60.
7 J. Liu and R. J. Linhardt, *Nat. Prod. Rep.*, 2014, **31**, 1676.
8 S. Park, J. C. Gildersleeve, O. Blixt and I. Shin, *Chem. Soc. Rev.*, 2013, **42**, 4310.
9 Y. Liu, A. S. Palma and T. Feizi, *Biol. Chem.*, 2009, **390**, 647.
10 D. F. Smith and R. D. Cummings, *Curr. Opin. Virol.*, 2014, **7**, 79.
11 S. R. Stowell, C. M. Arthur, R. McBride, O. Berger, N. Razi, J. Heimburg-Molinaro, L. C. Rodrigues, J.-P. Gourdine, A. J. Noll, S. von Gunten, D. F. Smith, Y. A. Knirel, J. C. Paulson and R. D. Cummings, *Nat. Chem. Biol.*, 2014, **10**, 470.
12 J. Pai, J. Y. Hyun, J. Jeong, S. Loh, E.-H. Cho, Y.-S. Kang and I. Shin, *Chem. Sci.*, 2016, **7**, 2084.
13 X. Song, H. Ju, Y. Lasanajak, M. R. Kudelka, D. F. Smith and R. D. Cummings, *Nat. Methods*, 2016, **13**, 528.
14 X. Song, Y. Lasanajak, B. Xia, J. Heimburg-Molinaro, J. M. Rhea, H. Ju, C. Zhao, R. J. Molinaro, R. D. Cummings and D. F. Smith, *Nat. Methods*, 2011, **8**, 85.
15 Z. Wang, Z. S. Chinoy, S. G. Ambre, W. Peng, R. McBride, R. de Vries, J. Glushka, J. C. Paulson and G.-J. Boons, *Science*, 2013, **341**, 379.
16 Z. Xiao, Y. Guo, Y. Liu, L. Li, Q. Zhang, L. Wen, X. Wang, S. M. Kondengaden, Z. Wu, J. Zhou, X. Cao, X. Li, C. Ma and P. G. Wang, *J. Org. Chem.*, 2016, **81**, 5851.
17 K. Brzezicka, B. Echeverria, S. Serna, A. van Diepen, C. H. Hokke and N.-C. Reichardt, *ACS Chem. Biol.*, 2015, **10**, 1290.
18 C. Gama, S. E. Tully, N. Sotogaku, P. M. Clark, M. Rawat, N. Vaidehi, W. A. Goddard, A. Nishi and L. C. Hsieh-Wilson, *Nat. Chem. Biol.*, 2006, **2**, 467.
19 T. Puvirajesinghe, Y. Ahmed, A. Powell, D. Fernig, S. Guimond and J. E. Turnbull, *Chem. Biol.*, 2012, **19**, 553.
20 E. Shipp and L. C. Hsieh-Wilson, *Chem. Biol.*, 2007, **14**, 195.
21 J. L. de Paz, C. Noti and P. H. Seeberger, *J. Am. Chem. Soc.*, 2006, **128**, 2766.
22 J. L. de Paz, E. A. Moseman, C. Noti, L. Polito, U. H. von Andrian and P. H. Seeberger, *ACS Chem. Biol.*, 2007, **2**, 735.
23 S. B. Dulaney, Y. Xu, P. G. Wang, G. Tiruchinapally, Z. Wang, J. Kathawa, M. H. El-Dakdouki, B. Yang, J. Liu and X. Huang, *J. Org. Chem.*, 2015, **80**, 12265.
24 Y. Xu, S. Masuko, M. Takieddin, H. Xu, R. Liu, J. Jing, S. A. Mousa, R. J. Linhardt and J. Liu, *Science*, 2011, **334**, 498.
25 Y. Xu, C. Cai, K. Chandarajoti, P. Hsieh, Y. Lin, T. Q. Pham, E. M. Sparkenbaugh, J. Sheng, N. S. Key, R. L. Pawlinski, E. N. Harris, R. J. Linhardt and J. Liu, *Nat. Chem. Biol.*, 2014, **10**, 248.
26 M. Warda, T. Toida, F. Zhang, P. Sun, E. Munoz, J. Xie and R. J. Linhardt, *Glycoconjugate J.*, 2006, **23**, 555.
27 A. Weyers, B. Yang, D. S. Yoon, J. H. Park, F. Zhang, K. B. Lee and R. J. Linhardt, *OMICS*, 2012, **16**, 79.
28 G. Li, L. Li, F. Tian, L. Zhang, C. Xue and R. J. Linhardt, *ACS Chem. Biol.*, 2015, **10**, 1303.
29 S. C. Edavettal, K. Carrick, R. R. Shah, L. C. Pedersen, A. Tropsha, R. M. Pope and J. Liu, *Biochemistry*, 2004, **43**, 4680.
30 A. F. Moon, Y. Xu, S. Woody, J. M. Krahn, R. J. Linhardt, J. Liu and L. C. Pedersen, *Proc. Natl. Acad. Sci. U. S. A.*, 2012, **109**, 5256.
31 D. H. Atha, J.-C. Lormeau, M. Petitou, R. D. Rosenberg and J. Choay, *Biochemistry*, 1985, **24**, 6723.
32 U. Lindahl, G. Backstrom, M. Hook, L. Thunberg, L. A. Fransson and A. Linker, *Proc. Natl. Acad. Sci. U. S. A.*, 1979, **76**, 3198.

